# Disorder enhanced quantum many-body scars in Hilbert hypercubes

Van Voorden, B.; Marcuzzi, M.; Schoutens, K.; Minář, J.

**DOI**
10.1103/PhysRevB.103.L220301

**Publication date**
2021

**Document Version**
Final published version

**Published in**
Physical Review B

Letter

# Disorder enhanced quantum many-body scars in Hilbert hypercubes

Bart van Voorden [1], Matteo Marcuzzi [2], Kareljan Schoutens [1,3] and Jiří Minář [1,3]
[1] Institute for Theoretical Physics, University of Amsterdam, Science Park 904, 1098 XH Amsterdam, The Netherlands
[2] School of Physics and Astronomy, University of Nottingham, Nottingham NG7 2RD, United Kingdom
[3] QuSoft, Science Park 123, 1098 XG Amsterdam, The Netherlands

(Received 11 December 2020; revised 4 May 2021; accepted 17 May 2021; published 3 June 2021)

We consider a model arising in facilitated Rydberg chains with positional disorder which features a Hilbert space with the topology of a $d$-dimensional hypercube. This allows for a straightforward interpretation of the many-body dynamics in terms of a single-particle one on the Hilbert space and provides an explicit link between the many-body and single-particle scars. Exploiting this perspective, we show that an integrability-breaking disorder enhances the scars followed by inhibition of the dynamics due to strong localization of the eigenstates in the large disorder limit. Next, mapping the model to the spin-1/2 XX Heisenberg chain offers a simple geometrical perspective on the recently proposed Onsager scars [Phys. Rev. Lett. **124**, 180604 (2020)], which can be identified with the scars on the edge of the Hilbert space. This makes apparent the origin of their insensitivity to certain types of disorder perturbations.

DOI: 10.1103/PhysRevB.103.L220301

*Introduction.* The understanding of thermalization and relaxation dynamics is at the forefront of research on quantum many-body systems out of equilibrium. Since the formulation of the eigenstate thermalization hypothesis [1–3], predicting fast thermalization following a quench from most many-body states, many exceptions to this behavior have been identified. The prominent examples are integrable [4,5] and many-body localized (MBL) systems [6–14]. A recently added category is quantum many-body scars (QMBS) [15,16], which are particular eigenstates responsible for slow decay and oscillatory behavior of observables following a quantum quench from certain initial states, typically close to a product state, as observed in Ref. [17] realizing the so-called PXP model [18]. This has triggered a great interest in QMBS in settings ranging from constrained to driven [19–64], and recently also disordered systems [65,66].

QMBS owe their name to the single-particle quantum scars [67,68] which were in turn inspired by particle motion in classical billiards. In both the quantum and classical cases, it is the shape of the billiard boundary, such as the celebrated Bunimovich stadium or cardioid shape [69,70], which causes the motion of the particle to be generically ergodic. The exception to this rule is a set of periodic trajectories, around which the density of certain wave functions—the scars—is enhanced in the quantum case.

Here we analyze a model of spins-1/2, which describes a chain of Rydberg atoms with open boundaries under a facilitation condition [71]. Representing the Hilbert space as a graph, we show that it corresponds to a truncated hypercube with the dimension given by the number of spin clusters (cf. below for definition).

This allows us to identify the QMBS as single-particle scars on the Hilbert space [16]. Building on the graph representation of the Hilbert space, an approach also exploited in the studies of MBL [6,7,32,72–77], we demonstrate that the scar signatures are *enhanced* in the presence of disorder, naturally emerging from the positional disorder of the atoms. Finally, exploiting the mapping of the present model to the Heisenberg spin-1/2 XX chain [78], we identify the recently proposed Onsager scars [65,79] with scars corresponding to sparse eigenstates residing at the "edge" of the Hilbert space. This provides intriguing connections between QMBS and single-particle scars and highlights the utility of a graph-theoretical approach to many-body dynamics, which has been advocated also in the studies of quantum chaos [80–84], integrability [85], QMBS [86], and fermionic and exchange models [87,88].

*The model.* We consider a one-dimensional chain of $M$ Rydberg atoms along the $z$ axis, with open boundaries and spaced by $r_0$. We denote the ground and excited (Rydberg) states as $|{\downarrow}\rangle, |{\uparrow}\rangle$. The corresponding Hamiltonian reads

$$H_{\mathrm{Ry}} = \sum_k \frac{\Omega}{2}\sigma_k^x + \Delta n_k + \sum_{l>k} V(|\mathbf{r}_k - \mathbf{r}_l|) n_k n_l, \tag{1}$$

where $\sigma_k^x = |{\uparrow_k}\rangle\langle{\downarrow_k}| + |{\downarrow_k}\rangle\langle{\uparrow_k}|$, $n_k = |{\uparrow_k}\rangle\langle{\uparrow_k}|$, and $V(r) = C_\alpha/r^\alpha$, $r = |\mathbf{r}|$. $C_\alpha$, which we take to be positive, is the interaction strength coefficient with $\alpha = 3\,(6)$ for dipole-dipole (van der Waals) interaction. The positions of the atoms are $\mathbf{r}_k = (0, 0, (k-1)r_0) + \delta\mathbf{r}_k$, where $\delta\mathbf{r}_k$ describes the positional disorder which induces the disorder in energy. Denoting $V_{\mathrm{NN}} = V(r_0)$ and $V_{\mathrm{NNN}} = V(2r_0)$, we define an energy shift for a pair of nearest neighbors $\delta V_k = V_{\mathrm{NN}} - V(|\mathbf{r}_{k+1} - \mathbf{r}_k|)$.

It has been shown in [71] that under the facilitation condition $\Delta = -V_{\mathrm{NN}}$ and in the regime $V_{\mathrm{NN}} \gg \Omega, \delta V_k$ the Hamiltonian (1) effectively reduces to

$$H_{\mathrm{eff}} = \Delta N_{\mathrm{cl}} + \sum_k \frac{\Omega}{2}\sigma_k^x P_{\langle k\rangle} + \delta V_k n_k n_{k+1} + V_{\mathrm{NNN}} n_k n_{k+2}, \tag{2}$$

 

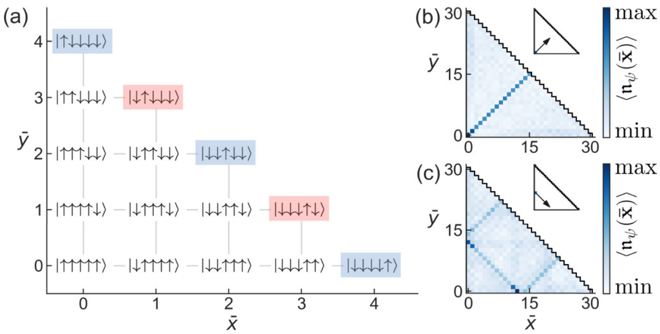


FIG. 1. (a) Hilbert space structure for $M = 5$ in the $N_{\rm cl} = 1$ sector. The (blue, red) boxes highlight the respective phases $(-, +)$ of basis states constituting a specific sparse eigenvector (a scar). (b),(c) The occupation Eq. (9) with $(\Omega\tau_0, \Omega\tau_1) = (175, 700)$ for a quench from the initial state Eq. (8) with $w = 2$ and the initial momenta $\mathbf{p}$ and positions $\bar{\mathbf{x}}_0$ indicated in the insets.

where $P_{\langle k\rangle} = n_{k-1} + n_{k+1} - 2n_{k-1}n_{k+1}$ and $N_{\rm cl} = \sum_k n_k(1 - n_{k+1})$, $n_0 = n_{N+1} = 0$, denotes the number of clusters, which are blocks of consecutive spin excitations (e.g., the configuration $\downarrow\downarrow \boxed{\uparrow\uparrow} \downarrow \boxed{\uparrow\uparrow\uparrow}$ contains two clusters highlighted by boxes). The projector $P_{\langle k\rangle}$ ensures the clusters cannot merge or disappear and hence their number represents a conserved charge, $[N_{\rm cl}, H_{\rm eff}] = 0$. For each $N_{\rm cl}$, the topology of the Hilbert subspace of (2) is that of a truncated hypercube of dimension $d = 2N_{\rm cl}$ [89].

In what follows we will be particularly focusing on the $N_{\rm cl} = 1$ sector for which the Hilbert space can be represented as a square lattice with a triangular boundary. Each site $(\bar{x}, \bar{y})$ of this lattice corresponds to a state

$$|\bar{\mathbf{x}}\rangle \equiv |\bar{x}, \bar{y}\rangle = |[\downarrow]_{\bar{x}} \uparrow \cdots \uparrow [\downarrow]_{\bar{y}}\rangle\,. \tag{3}$$

Here, $[\downarrow]_\ell$ labels a string of consecutive down spins of length $\ell$. The boundaries are determined by the natural conditions $x \geqslant 0$, $y \geqslant 0$, and $x + y < M$ [cf. Fig. 1(a)].

$H_{\rm eff}$ projected on the $N_{\rm cl} = 1$ sector can be written as

$$H = H_0 + H_{\rm pot} + H_{\rm dis}, \tag{4a}$$

$$H_0 = \frac{\Omega}{2} \sum_{\bar{\mathbf{x}} \in \mathcal{H}\backslash b} |\bar{\mathbf{x}}\rangle(\langle\bar{\mathbf{x}} + 1_{\bar{x}}| + \langle\bar{\mathbf{x}} + 1_{\bar{y}}|) + \text{H.c.}, \tag{4b}$$

$$H_{\rm pot} = V_{\rm NNN} \sum_{\bar{\mathbf{x}} \in \mathcal{H}} \max\,[0, M - 2 - (\bar{x} + \bar{y})]|\bar{\mathbf{x}}\rangle\langle\bar{\mathbf{x}}|, \tag{4c}$$

$$H_{\rm dis} = \sum_{\bar{\mathbf{x}} \in \mathcal{H}} |\bar{\mathbf{x}}\rangle\,\langle\bar{\mathbf{x}}|\,\delta V_{\bar{\mathbf{x}}}, \tag{4d}$$

where $1_{\bar{x},\bar{y}}$ are unit vectors in the direction $\bar{x}, \bar{y}$, $\mathcal{H} = \{|\bar{\mathbf{x}}\rangle\,|0 \leqslant (\bar{x}, \bar{y}) < M \wedge \bar{x} + \bar{y} < M\}$, $b = \{|\bar{\mathbf{x}}\rangle\,|\bar{x} + \bar{y} = M - 1\}$, and $\delta V_{\bar{\mathbf{x}}}$ is specified in Eq. (10).

$H_0$ can be solved exactly [89] with eigenenergies

$$2\Omega^{-1}E_{m,n} = 2\cos\left(\frac{m\pi}{M+2}\right) + 2\cos\left(\frac{n\pi}{M+2}\right) \tag{5}$$

and eigenvectors

$$|w_{m,n}\rangle = \sum_{\mathsf{x},\mathsf{y}}[u_m(\mathsf{x})u_n(-\mathsf{y}) - u_m(-\mathsf{y})u_n(\mathsf{x})]|\mathsf{x}, \mathsf{y}\rangle, \tag{6}$$

where

$$u_m(\mathsf{x}) = \sqrt{\frac{2}{M+2}}\sin\left[\frac{\pi m}{M+2}\left(\mathsf{x} + 1 + \frac{M}{2}\right)\right]. \tag{7}$$

In Eqs. (6) and (7) we have used the shifted variables $\mathsf{x} = \bar{x} - M/2$, $m, n \in \{1, 2, \ldots, M+1\}$, $m > n$, and $\bar{\mathbf{x}} \in \mathcal{H}$. All energies are nondegenerate, except for $\lceil M/2 \rceil$ zero-energy states for which $m + n = M + 2$. It can be shown that the zero-energy subspace is spanned by eigenvectors, which are sparse in the basis Eq. (3) [89]. Due to its simple structure, these states can be identified as scars in the Hilbert space [cf. Fig. 1(a)]. Consequently, one can directly apply the single-particle perspective used in quantum scars on discrete lattices [90]. In what follows we examine the dynamics following a quantum quench. Motivated by the use of Gaussian wave packets as probes for single-particle scars [67,68,91,92], we introduce effective "Gaussian" initial states defined as (up to normalization)

$$\left|\psi_{\bar{\mathbf{x}}_0}^{\mathbf{p},w}(t=0)\right\rangle \propto \mathcal{P}\sum_{\bar{\mathbf{x}}} \mathrm{e}^{-[(\bar{\mathbf{x}}-\bar{\mathbf{x}}_0)^2/2w^2]} e^{-i\mathbf{p}\cdot\bar{\mathbf{x}}}\,|\bar{\mathbf{x}}\rangle\,, \tag{8}$$

where $\mathbf{p} = (p_x, p_y)$ are the phases specifying the initial direction of propagation of the "wave packet" and for simplicity we project the state by $\mathcal{P}$ on four basis states with maximal weight. For future convenience, we define $|\psi_G\rangle \equiv |\psi_{\bar{\mathbf{x}}_0=(0,0)}^{\mathbf{p}=(\pi/2,\pi/2),w=2}\rangle$. We also define the time-averaged occupation of the basis states in the Hilbert space as

$$\langle \mathrm{n}_\psi(\bar{\mathbf{x}})\rangle = \frac{1}{\tau_1 - \tau_0}\int_{\tau_0}^{\tau_1} dt\,|\langle\bar{\mathbf{x}}|\psi(t)\rangle|^2, \tag{9}$$

where $|\psi(t)\rangle$ is the time evolved initial state.

In Figs. 1(b) and 1(c) we show $\langle \mathrm{n}_\psi(\bar{\mathbf{x}})\rangle$ for different initial states Eq. (8). It is apparent that the occupation reveals the scar behavior in the Hilbert space in exact analogy to the single-particle case.

*Disorder.* Since $H_0$ is integrable, a natural way to break the integrability is provided by positional disorder of the atoms. Denoting $\delta\mathbf{r}_k = (x_k, y_k, z_k)$, the initial position of the $k$th atom is drawn from a Gaussian probability distribution $p(\delta\mathbf{r}_k) = (2\pi)^{-3/2}(\prod_{\nu=x,y,z}\sigma_\nu)^{-1}\exp[-\sum_{\nu=x,y,z}\frac{\nu_k^2}{2\sigma_\nu^2}]$ [71,93,94].

While the primary focus of this Letter is the analysis of the model (2),(1), to provide a description applicable to a realistic experimental realization, the time dependence of the atom motion $\mathbf{r}_k(t)$ has to be taken into account. To set the stage, a few remarks are in order.

First, we consider both the ground and the Rydberg states to be subject to the same harmonic trapping potential $H_{\rm tr} = \sum_k\sum_{\nu=x,y,z} m\omega_\nu^2\nu_k^2/2$ [95], where $\omega_\nu$ are the trap frequencies which determine, together with the inverse temperature $\beta = 1/k_{\rm B}T$, the disorder through $\sigma_\nu = \sqrt{1/(\beta m\omega_\nu^2)}$ and $m$ is the atom mass. We parametrize the trap frequencies as $\boldsymbol{\omega} = (\epsilon^{-1}, 1, 1)\omega_0/d$, which leads to the dimensionless disorder $\mathbf{s} = (s_x, s_y, s_z) \equiv (\epsilon, 1, 1)ds_0$, where $s_0 = \sigma_0/r_0$ for some $\sigma_0$ and motivated by [71] we choose $s_0 = 0.03$. Here $\epsilon$ and $d$ tune the shape and the overall strength of the trapping potential where typically $\epsilon > 1$ in a tweezer experiment [71,78,93].

Second, we note that the interaction $V(|\mathbf{r}_k - \mathbf{r}_l|)$ leads to dynamics entangling the motional and internal degrees of freedom necessitating a fully quantum treatment. This is a difficult problem limiting the applicability of methods such as exact diagonalization to few sites and small phonon number [96]. To proceed, we treat the atomic motion $\mathbf{r}_k(t)$ as that of a classical particle in a harmonic potential with coordinates $\nu_k(t) = C_{\nu,k}\cos(\omega_\nu t + \phi_{\nu,k})$, where $C_{\nu,k} = \sqrt{\nu_k(0)^2 + [q_{\nu,k}(0)/m]^2/\omega_\nu^2}$ and $\phi_{\nu,k} = \arccos[\nu_k(0)/C_{\nu,k}]$, which are fully specified by the initial position $\nu_k(0) = \delta r_{k,\nu}(t=0)$ and momentum $q_{\nu,k}(0)$. Here, the latter is drawn from an isotropic Boltzmann distribution $p(q_{\nu,k}) \propto \exp[-\beta q_{\nu,k}^2/(2m)]$.

The third and final comment is that for $V \propto 1/r^\alpha$, the distribution $p(\delta\mathbf{r}_k)$ leads to the energy probability distribution $p(\delta V)$ with undefined moments, a consequence of rare events when two atoms come arbitrarily close to each other [93]. This is an artifact, not expected to occur under realistic experimental conditions, of the algebraic form of $V$. For this reason and in order to gain analytical control, we use a small-displacement approximation

$$\begin{aligned}\delta V_{\bar{\mathbf{x}}} &= \sum_{k=\bar{x}+1}^{M-\bar{y}-1}\left[\frac{C_\alpha}{|\mathbf{r}_{k+1}-\mathbf{r}_k|^\alpha} - V_{\mathrm{NN}}\right]\\ &\approx -\sum_{k=\bar{x}+1}^{M-\bar{y}-1}\alpha V_{\mathrm{NN}}\left[\tilde{\delta}_{z,k} + \frac{1}{2}\left(\tilde{\delta}_{x,k}^2 + \tilde{\delta}_{y,k}^2 - (1+\alpha)\tilde{\delta}_{z,k}^2\right)\right],\end{aligned} \tag{10}$$

where $\tilde{\delta}_{\nu,k} = (\nu_{k+1} - \nu_k)/r_0$. In order to get the occupation (9) with the time-dependent Hamiltonian (4a), we solve the corresponding Schrödinger equation for the wave function. In particular, we are interested in the properties of the occupation as a function of the disorder. The results for $|\psi(0)\rangle = |\psi_G\rangle$ are shown in Figs. 2(a) and 2(f) with examples of $\langle \mathfrak{n}_{\psi_G}(\bar{\mathbf{x}})\rangle$

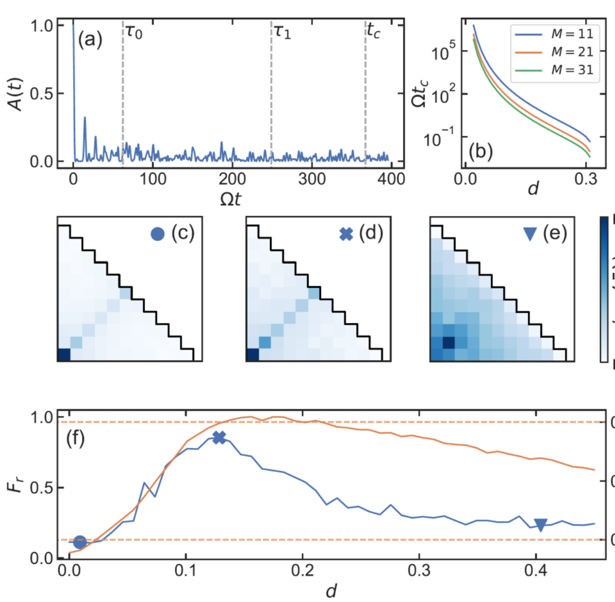


FIG. 2. (a) An example of the autocorrelation $A(t) = |\langle\psi_G|\psi(t)\rangle|^2$ for $M = 11$. (b) The threshold time $t_c$ vs disorder strength for various system sizes $M$. (c)–(e) Examples of the occupation Eq. (9) for various disorder strengths indicated by circle, cross, and triangle, respectively, in panel (f). (f) $F_r$ (blue) and the $r$ statistics (orange) vs disorder strength $d$ [here $\alpha = 6$, $s_0 = 0.03$, $\epsilon = 9$, $(\Omega\tau_0, \Omega\tau_1) = (50, 250)$ and $V_{\mathrm{NN}}/\Omega = 4$].

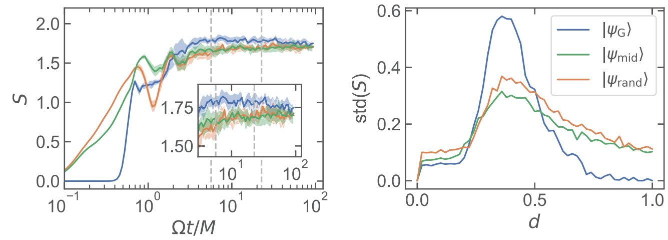


FIG. 3. (a) Evolution of half-chain entanglement entropy $S$ for $d = 0.12$ and $M = 25$ following a quench from $|\psi_{\mathrm{G}}\rangle$ (blue), $|\psi_{\mathrm{rand}}\rangle$ (green), and $|\psi_{\mathrm{mid}}\rangle$ (orange). The vertical dashed lines indicate the (scaled) times $\tau_0$, $\tau_1$ used in Fig. 2 and the inset shows the detail of the late-time evolution. (b) The standard deviation of the saturated $S$ vs $d$. Data obtained with 10 realizations of the initial conditions (a) and 300 realizations (b), where static disorder was considered for numerical reasons, yielding a value of the average saturated entropy compatible with (a) within std$[S(t\to\infty)]$.

for three different values of disorder shown in Figs. 2(c)–2(e). The solid blue line in Fig. 2(f) corresponds to a quantity $F_r$ which characterizes the overlap of the occupation with the occupation $\langle\mathfrak{n}_\psi(\bar{\mathbf{x}})\rangle_0$ generated by the idealized Hamiltonian $H_0$, Eq. (4b). It is defined as $F_r = (F - F_u)/(1 - F_u)$, where $F = \sum_{\bar{\mathbf{x}}}\langle\langle\tilde{\mathfrak{n}}_\psi(\bar{\mathbf{x}})\rangle\rangle\,\langle\langle\tilde{\mathfrak{n}}_\psi(\bar{\mathbf{x}})\rangle\rangle_0$, $F_u$ is given by $F$ with the replacement $\langle\tilde{\mathfrak{n}}_\psi(\bar{\mathbf{x}})\rangle \to \sqrt{2/(M+1)M}$, the tilde denotes the occupations normalized as $\sum_{\bar{\mathbf{x}}}\langle\langle\tilde{\mathfrak{n}}_\psi(\bar{\mathbf{x}})\rangle\rangle^2 = 1$, and the double angular brackets denote the averaging over disorder realizations (initial conditions). The rationale behind $F_r$ is that $F_r = 1$ when the occupation is that of the idealized scenario of Fig. 1(b) and $F_r = 0$ for a featureless uniform occupation. For comparison, the orange solid line shows the level statistics $r = \langle\langle\frac{\min(\Delta E_i, \Delta E_{i+1})}{\max(\Delta E_i, \Delta E_{i+1})}\rangle\rangle$ taking the initial conditions, i.e., quenched positional disorder, where the average is taken over all energy differences $\Delta E_i = E_i - E_{i-1}$ of adjacent ordered eigenenergies $E_i \geqslant E_{i-1}$ of $H$. The values $r \approx 0.39, 0.53$ corresponding to the Poisson and Wigner-Dyson statistics are indicated by the horizontal dashed lines. It is apparent from Fig. 2 that increasing the disorder *enhances* the many-body scars appearing in the occupation, which can be explained in terms of the eigenstate localization: as the disorder is increased from zero, the eigenstates of $H$ become more and more localized on the Hilbert space square lattice. This initially enhances their overlap with the initial state along the scar path. We observe similar enhancement also for other initial states and values of disorder and discuss quantitatively the energy landscape of the Hilbert space in [89].

*Thermalization.* Next we investigate how the scars affect the capacity of the system to thermalize. To this end we consider the time evolution of the (second Rényi) entanglement entropy (EE) $S(t) = -\log\mathrm{Tr}[\rho_A(t)^2]$, where $\rho_A(t)$ is the reduced density matrix of subsystem $A$, which we choose to be a half-chain of length $\lfloor\frac{M}{2}\rfloor$. In Fig. 3(a) we plot the time evolution of EE for a quench in the nonintegrable regime $d = 0.12$ from the Gaussian state $|\psi_{\mathrm{G}}\rangle$ (blue), a midspectrum eigenstate $|\psi_{\mathrm{mid}}\rangle$ of $H$ (orange), and a random state $|\psi_{\mathrm{rand}}\rangle \propto \sum_{\bar{\mathbf{x}}} c_{\bar{\mathbf{x}}}\,|\bar{\mathbf{x}}\rangle$ (green), where $c_{\bar{\mathbf{x}}}$ are drawn from a uniform random distribution. Here, $|\psi_{\mathrm{mid}}\rangle$ and $|\psi_{\mathrm{rand}}\rangle$ are defined on the half-chain so that $S(0) = 0$. After the initial rise we observe a slow growth (cf. [89] for extended discussion) for all the states which we attribute to superscarring, i.e., the fact that *each* basis state either belongs to a scar in the Hilbert space or is adjacent to it. We also note the initial rise for the Gaussian state happening for $\Omega t \approx M/2$, which corresponds to the geometrical distance from the tip [$\bar{\mathbf{x}} = (0, 0)$] to the base of the triangular-shaped Hilbert space [cf. Fig. 1(a)]. We note that the scar enhancement is not reflected in the standard deviation of the saturated entropy std[$S(t \to \infty)$] shown in Fig. 3(b), where the dominant peak around $d \approx 0.3$ corresponds to the transition from nonintegrable to integrable as quantified by $r$ [13,75,97] and hints towards a possible MBL-like phase [78].

*Relation to Onsager scars.* It has been shown in [78] that the spin flip part of $H_{\rm eff}$, Eq. (2), can be mapped to the spin-1/2 XX Heisenberg spin chain of length $M+1$

$$\sum_k \sigma_k^x P_{\langle k\rangle} \to H_{\rm XX} = \sum_{k=1}^{M} \mu_k^x \mu_{k+1}^x + \mu_k^y \mu_{k+1}^y, \tag{11}$$

where $\mu^{x,y,z}$ are the Pauli matrices in a $\{|0\rangle, |1\rangle\}$ basis. It is related to the $\{|\downarrow\rangle, |\uparrow\rangle\}$ basis through the mapping $\uparrow\uparrow, \downarrow\downarrow \to 0$, $\uparrow\downarrow, \downarrow\uparrow \to 1$, where the ambiguity is lifted by including fictitious boundary spins ($\downarrow$) to the left and right ends of the chain. Consequently, $\sigma_k^x = \mu_k^x \mu_{k+1}^x$, $\sigma_k^y = (-1)^{k+1} \prod_{l=1}^{k-1} \mu_l^z \mu_k^y \mu_{k+1}^x$, $\sigma_k^z = (-1)^{k+1} \prod_{l=1}^{k} \mu_l^z$, and $\delta V$ of Eq. (2) maps to nonlocal disorder given by a string of $\mu^z$ operators [78].

Crucially, the structure of the Hilbert space (connectivity between the basis states) remains unchanged as it is given solely by the spin flip terms [89]. Recently, Ref. [65] proposed a class of spin models with $n$ spin components featuring so-called Onsager scars, which are states with perfect revivals of the integrated autocorrelation subject to certain types of integrability-breaking disorder. The simplest instance $n = 2$ of this class is $H_{\rm XX}$, Eq. (11), with the Onsager scar $|\psi(\beta)\rangle \propto \exp[\beta^2 Q^+] |0\ldots0\rangle = \sum_{N_{\rm cl}=0}^{\lceil (M+1)/2 \rceil} \frac{(\beta^2 Q^+)^{N_{\rm cl}}}{N_{\rm cl}!} |0\ldots0\rangle$ and $Q^+ = \sum_k (-1)^{k+1} \mu_k^+ \mu_{k+1}^+$. We have intentionally indexed the summation in the definition of $|\psi(\beta)\rangle$ by $N_{\rm cl}$ as each term corresponds to a superposition of $N_{\rm cl}$ pairs $|\ldots 1_k 1_{k+1} \ldots\rangle$, i.e., *single* Rydberg spins $\uparrow$. The projection of $|\psi(\beta)\rangle$ on the $N_{\rm cl} = 1$ sector is nothing but the scar indicated in Fig. 1(a).

This allows for the following identifications: (i) The $\lceil (M+1)/2 \rceil$ eigenstates which form the special band in the plot of the eigenstates' EE [cf. Fig. 2(a) in [65]] correspond to different cluster sectors of $H_{\rm eff}$. (ii) The projection of $|\psi(\beta)\rangle$ on the $N_{\rm cl} = 1$ sector is the scar corresponding to the $(0, M-1) - (M-1, 0)$ diagonal, i.e., the *edge* of the Hilbert space [cf. Fig. 1(a)], which is comprised only of single Rydberg spin excitations. This interpretation applies to other $N_{\rm cl}$ as well. Furthermore, the simple structure of the Hilbert space allows for a straightforward visualization of why certain types of the integrability-breaking disorder do not affect the Onsager scars, such as Eq. (13) in [65]. Another example naturally realized in the Rydberg systems is the disorder of Eq. (2), which affects all but the isolated Rydberg spins.

*Experimental considerations.* We have simulated the time evolution with the assumption that the atomic trajectories are that of classical particles in a harmonic potential, independent of their internal state. To estimate the effect of the Rydberg interactions on the atomic motion and hence the disorder energies, we consider $\langle \delta V(n_{\rm NN}) \rangle$ to be the expectation value of $\delta V_{\bar{\mathbf{x}}}$, Eq. (10), corresponding to basis state $|\bar{\mathbf{x}}\rangle$ containing $n_{\rm NN}$ nearest neighbors and evaluated using $p(\delta \mathbf{r}_k)$. Analogously, we define $\langle \delta V(n_{\rm NN}) \rangle_{\rm int}$ where the equilibrium positions of the atoms are taken in the presence of the interactions [89]. The difference between the two provides an estimate for a threshold timescale beyond which the atomic motion cannot be treated as independent of the internal state and we define $t_c \equiv 2\pi\hbar/(\langle \delta V(M-1)\rangle_{\rm int} - \langle \delta V(M-1)\rangle)$. The plot of $t_c$ vs $d$ is shown in Fig. 2(b) with an example of $t_c$ indicated in Fig. 2(a). Thus, for $d \approx 0.1$, the present analysis holds for $\Omega t = O(100)$ for $M$ of few tens, sufficient to capture the behavior of the time-averaged occupation in a realistic experimental setting.

*Outlook.* In this work we have highlighted how the structure of the Hilbert space, resembling that of a hypercube, provides useful insights in the nonequilibrium dynamics in spin chains. This allowed us to identify quantum many-body scars as single-particle scars in the Hilbert space, link them to the Onsager scars, and show how their signature is enhanced by disorder. This provides a number of interesting openings, such as the interpretation of the disordered Heisenberg XXZ spin chain as that of an Anderson model on a hypercubic lattice, which is relevant to the ongoing discussion about the scaling of the Thouless time in many-body systems [98,99]. It would also be interesting to explore the role of sparse eigenvectors, which play an important role in various applications, such as in the signal analysis of networks [100,101], in the context of many-body Hamiltonians and their graph-theoretic representations [85,87,88,102]. Finally, to describe the entangling dynamics between the motional and internal degrees of freedom, new approaches, such as the variational ansatz based on non-Gaussian states [103], need to be investigated.

*Acknowledgments.* We are very grateful to V. Gritsev, Neil J. Robinson, W. Buijsman, W. Vleeshouwers, A. Urech, V. Alba, T. Iadecola, Y. Miao, and O. Gamayun for fruitful discussions. This work is part of the Delta ITP consortium, a program of the Netherlands Organisation for Scientific Research (NWO) that is funded by the Dutch Ministry of Education, Culture and Science (OCW). M.M. gratefully acknowledges funding from the University of Nottingham under a Nottingham Research Fellowship scheme.

[1] J. M. Deutsch, Phys. Rev. A **43**, 2046 (1991).
[2] M. Srednicki, Phys. Rev. E **50**, 888 (1994).
[3] M. Rigol, V. Dunjko, and M. Olshanii, Nature (London) **452**, 854 (2008).
[4] B. Sutherland, *Beautiful Models: 70 Years of Exactly Solved Quantum Many-Body Problems* (World Scientific, Singapore, 2004).
[5] M. Takahashi, *Thermodynamics of One-Dimensional Solvable Models* (Cambridge University Press, Cambridge, UK, 2005).
[6] I. V. Gornyi, A. D. Mirlin, and D. G. Polyakov, Phys. Rev. Lett. **95**, 206603 (2005).
[7] D. M. Basko, I. L. Aleiner, and B. L. Altshuler, Ann. Phys. **321**, 1126 (2006).

[8] M. Serbyn, Z. Papić, and D. A. Abanin, Phys. Rev. Lett. **111**, 127201 (2013).
[9] D. A. Huse, R. Nandkishore, and V. Oganesyan, Phys. Rev. B **90**, 174202 (2014).
[10] R. Nandkishore and D. A. Huse, Annu. Rev. Condens. Matter Phys. **6**, 15 (2015).
[11] J. Z. Imbrie, J. Stat. Phys. **163**, 998 (2016).
[12] J. Z. Imbrie, V. Ros, and A. Scardicchio, Ann. Phys. **529**, 1600278 (2017).
[13] F. Alet and N. Laflorencie, C. R. Phys. **19**, 498 (2018).
[14] D. A. Abanin, E. Altman, I. Bloch, and M. Serbyn, Rev. Mod. Phys. **91**, 021001 (2019).
[15] C. J. Turner, A. A. Michailidis, D. A. Abanin, M. Serbyn, and Z. Papić, Phys. Rev. B **98**, 155134 (2018).
[16] C. J. Turner, A. A. Michailidis, D. A. Abanin, M. Serbyn, and Z. Papić, Nat. Phys. **14**, 745 (2018).
[17] H. Bernien, M. D. Lukin, H. Pichler, S. Choi, M. Greiner, V. Vuletić, A. Omran, H. Levine, S. Schwartz, A. Keesling, M. Endres, and A. S. Zibrov, Nature (London) **551**, 579 (2017).
[18] I. Lesanovsky and H. Katsura, Phys. Rev. A **86**, 041601(R) (2012).
[19] S. Choi, C. J. Turner, H. Pichler, W. W. Ho, A. A. Michailidis, Z. Papić, M. Serbyn, M. D. Lukin, and D. A. Abanin, Phys. Rev. Lett. **122**, 220603 (2019).
[20] C.-J. Lin and O. I. Motrunich, Phys. Rev. Lett. **122**, 173401 (2019).
[21] T. Iadecola, M. Schecter, and S. Xu, Phys. Rev. B **100**, 184312 (2019).
[22] T. Iadecola and M. Schecter, Phys. Rev. B **101**, 024306 (2020).
[23] F. M. Surace, P. P. Mazza, G. Giudici, A. Lerose, A. Gambassi, and M. Dalmonte, Phys. Rev. X **10**, 021041 (2020).
[24] C.-J. Lin, A. Chandran, and O. I. Motrunich, Phys. Rev. Res. **2**, 033044 (2020).
[25] K. Bull, J.-Y. Desaules, and Z. Papic, Phys. Rev. B **101**, 165139 (2020).
[26] D. K. Mark, C.-J. Lin, and O. I. Motrunich, Phys. Rev. B **101**, 094308 (2020).
[27] C.-J. Lin, V. Calvera, and T. H. Hsieh, Phys. Rev. B **101**, 220304 (2020).
[28] Y. Yang, S. Iblisdir, J. I. Cirac, and M. C. Bañuls, Phys. Rev. Lett. **124**, 100602 (2020).
[29] W. W. Ho, S. Choi, H. Pichler, and M. D. Lukin, Phys. Rev. Lett. **122**, 040603 (2019).
[30] K. Bull, I. Martin, and Z. Papić, Phys. Rev. Lett. **123**, 030601 (2019).
[31] N. Pancotti, G. Giudice, J. I. Cirac, J. P. Garrahan, and M. C. Bañuls, Phys. Rev. X **10**, 021051 (2020).
[32] S. Roy and A. Lazarides, Phys. Rev. Res. **2**, 023159 (2020).
[33] S. Ok, K. Choo, C. Mudry, C. Castelnovo, C. Chamon, and T. Neupert, Phys. Rev. Res. **1**, 033144 (2019).
[34] V. Khemani, C. R. Laumann, and A. Chandran, Phys. Rev. B **99**, 161101(R) (2019).
[35] A. Hallam, J. G. Morley, and A. G. Green, Nat. Commun. **10**, 2708 (2019).
[36] D. Jansen, J. Stolpp, L. Vidmar, and F. Heidrich-Meisner, Phys. Rev. B **99**, 155130 (2019).
[37] S. Moudgalya, T. Devakul, C. W. von Keyserlingk, and S. L. Sondhi, Phys. Rev. B **99**, 094312 (2019).
[38] H. Wilming, M. Goihl, I. Roth, and J. Eisert, Phys. Rev. Lett. **123**, 200604 (2019).
[39] A. A. Michailidis, C. J. Turner, Z. Papić, D. A. Abanin, and M. Serbyn, Phys. Rev. X **10**, 011055 (2020).
[40] A. V. Andreev, A. G. Balanov, T. M. Fromhold, M. T. Greenaway, A. E. Hramov, W. Li, V. V. Makarov, and A. M. Zagoskin, npj Quantum Inf. **7**, 1 (2021).
[41] Y. Werman, arXiv:2001.06110.
[42] G. De Tomasi, D. Hetterich, P. Sala, and F. Pollmann, Phys. Rev. B **100**, 214313 (2019).
[43] V. Khemani and R. Nandkishore, Phys. Rev. B **101**, 174204 (2020).
[44] P. Sala, T. Rakovszky, R. Verresen, M. Knap, and F. Pollmann, Phys. Rev. X **10**, 011047 (2020).
[45] P. Karpov, R. Verdel, Y.-P. Huang, M. Schmitt, and M. Heyl, Phys. Rev. Lett. **126**, 130401 (2021).
[46] S. Moudgalya, S. Rachel, B. A. Bernevig, and N. Regnault, Phys. Rev. B **98**, 235155 (2018).
[47] S. Moudgalya, N. Regnault, and B. A. Bernevig, Phys. Rev. B **98**, 235156 (2018).
[48] N. Shiraishi, J. Stat. Mech. (2019) 083103.
[49] D. K. Mark, C.-J. Lin, and O. I. Motrunich, Phys. Rev. B **101**, 195131 (2020).
[50] S. Moudgalya, E. O'Brien, B. A. Bernevig, P. Fendley, and N. Regnault, Phys. Rev. B **102**, 085120 (2020).
[51] S. Chattopadhyay, H. Pichler, M. D. Lukin, and W. W. Ho, Phys. Rev. B **101**, 174308 (2020).
[52] M. Schecter and T. Iadecola, Phys. Rev. Lett. **123**, 147201 (2019).
[53] T. Iadecola and M. Žnidarič, Phys. Rev. Lett. **123**, 036403 (2019).
[54] K. Lee, R. Melendrez, A. Pal, and H. J. Changlani, Phys. Rev. B **101**, 241111 (2020).
[55] Y. Chen and Z. Cai, Phys. Rev. A **101**, 023611 (2020).
[56] S. Sinha and S. Sinha, Phys. Rev. Lett. **125**, 134101 (2020).
[57] D. Villasenor, S. Pilatowsky-Cameo, M. A. Bastarrachea-Magnani, S. Lerma-Hernández, L. F. Santos, and J. G. Hirsch, New J. Phys. **22** 063036 (2020).
[58] S. Pai and M. Pretko, Phys. Rev. Lett. **123**, 136401 (2019).
[59] A. Pizzi, J. Knolle, and A. Nunnenkamp, Nat. Commun. **12**, 2341 (2021).
[60] S. Sugiura, T. Kuwahara, and K. Saito, Phys. Rev. Res. **3**, 012010 (2021).
[61] H. Zhao, J. Vovrosh, F. Mintert, and J. Knolle, Phys. Rev. Lett. **124**, 160604 (2020).
[62] B. Mukherjee, A. Sen, D. Sen, and K. Sengupta, Phys. Rev. B **102**, 014301 (2020).
[63] H. H. Jen, Phys. Rev. Res. **2**, 013097 (2020).
[64] C.-h. Fan, D. Rossini, H.-X. Zhang, J.-H. Wu, M. Artoni, and G. C. La Rocca, Phys. Rev. A **101**, 013417 (2020).
[65] N. Shibata, N. Yoshioka, and H. Katsura, Phys. Rev. Lett. **124**, 180604 (2020).
[66] I. Mondragon-Shem, M. G. Vavilov, and I. Martin, arXiv:2010.10535.
[67] L. Kaplan and E. J. Heller, Ann. Phys. **264**, 171 (1998).
[68] L. Kaplan, Nonlinearity **12**, R1 (1999).
[69] L. A. Bunimovich, Comm. Math. Phys. **65**, 295 (1979).
[70] M. Robnik, J. Phys. A **16**, 3971 (1983).

[71] M. Marcuzzi, J. Minář, D. Barredo, S. de Léséleuc, H. Labuhn, T. Lahaye, A. Browaeys, E. Levi, and I. Lesanovsky, Phys. Rev. Lett. **118**, 063606 (2017).
[72] B. L. Altshuler, Y. Gefen, A. Kamenev, and L. S. Levitov, Phys. Rev. Lett. **78**, 2803 (1997).
[73] C. Monthus and T. Garel, Phys. Rev. B **81**, 134202 (2010).
[74] A. De Luca and A. Scardicchio, Europhys. Lett. **101**, 37003 (2013).
[75] D. J. Luitz, N. Laflorencie, and F. Alet, Phys. Rev. B **91**, 081103(R) (2015).
[76] F. Pietracaprina, V. Ros, and A. Scardicchio, Phys. Rev. B **93**, 054201 (2016).
[77] S. Ghosh, A. Acharya, S. Sahu, and S. Mukerjee, Phys. Rev. B **99**, 165131 (2019).
[78] M. Ostmann, M. Marcuzzi, J. P. Garrahan, and I. Lesanovsky, Phys. Rev. A **99**, 060101(R) (2019).
[79] E. Vernier, E. O'Brien, and P. Fendley, J. Stat. Mech. (2019) 043107.
[80] T. Kottos and U. Smilansky, Ann. Phys. **274**, 76 (1999).
[81] H. Schanz and U. Smilansky, Phys. Rev. Lett. **84**, 1427 (2000).
[82] U. Smilansky, J. Phys. A **40**, F621 (2007).
[83] U. Smilansky, *Chaos* (Springer, New York, 2013), pp. 97–124.
[84] A. Lucas, arXiv:1903.01468.
[85] A. Chapman and S. T. Flammia, Quantum **4**, 278 (2020).
[86] A. Hudomal, I. Vasić, N. Regnault, and Z. Papić, Commun. Phys. **3**, 99 (2020).
[87] J. Decamp, J. Gong, H. Loh, and C. Miniatura, Phys. Rev. Res. **2**, 023059 (2020).
[88] J. Decamp, J. Gong, H. Loh, and C. Miniatura, Phys. Rev. Res. **2**, 033297 (2020).
[89] See Supplemental Material at http://link.aps.org/supplemental/10.1103/PhysRevB.103.L220301 for (i) diagonalization of $H_0$, (ii) the computation of disorder energy expectation values, (iii) the energy landscape, (iv) comments on the numerical treatment of the atomic motion, and (v) the structure of the Hilbert space and Refs. [104–114].
[90] V. Fernández-Hurtado, J. Mur-Petit, J. J. García-Ripoll, and R. A. Molina, New J. Phys. **16**, 035005 (2014).
[91] L. Kaplan and E. J. Heller, Phys. Rev. E **59**, 6609 (1999).
[92] D. A. Wisniacki, F. Borondo, E. Vergini, and R. M. Benito, Phys. Rev. E **62**, R7583 (2000).
[93] M. Ostmann, M. Marcuzzi, J. Minář, and I. Lesanovsky, Quantum Sci. Technol. **4**, 02LT01 (2019).
[94] H. Tamura, T. Yamakoshi, and K. Nakagawa, Phys. Rev. A **101**, 043421 (2020).
[95] J. Wilson, S. Saskin, Y. Meng, S. Ma, A. Burgers, and J. Thompson, arXiv:1912.08754.
[96] F. M. Gambetta, W. Li, F. Schmidt-Kaler, and I. Lesanovsky, Phys. Rev. Lett. **124**, 043402 (2020).
[97] J. A. Kjäll, J. H. Bardarson, and F. Pollmann, Phys. Rev. Lett. **113**, 107204 (2014).
[98] J. Šuntajs, J. Bonča, T. Prosen, and L. Vidmar, Phys. Rev. E **102**, 062144 (2020).
[99] P. Sierant, D. Delande, and J. Zakrzewski, Phys. Rev. Lett. **124**, 186601 (2020).
[100] O. Teke and P. P. Vaidyanathan, IEEE Trans. Signal Process. **65**, 5406 (2017).
[101] O. Teke and P. Vaidyanathan, in *2017 IEEE International Conference on Acoustics, Speech and Signal Processing (ICASSP)* (IEEE, New York, 2017), pp. 3904–3908.
[102] C.-F. Chen and A. Lucas, arXiv:1905.03682.
[103] T. Shi, E. Demler, and J. I. Cirac, Ann. Phys. **390**, 245 (2018).
[104] L. Losonczi, Acta Math. Hungarica **60**, 309 (1992).
[105] C. M. Da Fonseca and V. Kowalenko, Acta Math. Hungarica **160**, 376 (2019).
[106] C. M. da Fonseca and J. Petronilho, Numer. Math. **100**, 457 (2005).
[107] C. M. da Fonseca, Appl. Math. Lett. **19**, 1168 (2006).
[108] S. Kouachi, Electron. J. Linear Algebra **15**, 115 (2006).
[109] W.-C. Yueh, Appl. Math. E-Notes **5**, 66 (2005).
[110] E. Kılıç, Appl. Math. Comput. **197**, 345 (2008).
[111] D. Kulkarni, D. Schmidt, and S.-K. Tsui, Linear Algebra Appl. **297**, 63 (1999).
[112] R. K. Mallik, Linear Algebra Appl. **325**, 109 (2001).
[113] L. Banchi and R. Vaia, J. Math. Phys. **54**, 043501 (2013).
[114] B. Bollobás, *Modern Graph Theory* (Springer Science & Business Media, New York, 2013), Vol. 184.